Powder Technology 379 (2021) 641–654

Contents lists available at ScienceDirect

Powder Technology

journal homepage: www.elsevier.com/locate/powtec

Production of mixed rare earth oxide powder from a thorium containing complex Bastnasite ore

Sait Kursunoglu [a,*], Shokrullah Hussaini [b], Soner Top [a], Zela Tanlega Ichlas [c], Hasan Serkan Gokcen [b], Safak Ozsarac [d], Muammer Kaya [b]

[a] Abdullah Gul University, Department of Materials Science & Nanotechnology Engineering, Kayseri 38100, Turkey
[b] Eskisehir Osmangazi University, Department of Mining Engineering, Division of Mineral Processing, Eskisehir 26480, Turkey
[c] Institut Teknologi Bandung, Faculty of Mining and Petroleum Engineering, Department of Metallurgical Engineering, Bandung 40132, Indonesia
[d] Batman University, Department of Geological Engineering, Batman 72100, Turkey

ARTICLE INFO

Article history:
Received 27 June 2020
Received in revised form 15 September 2020
Accepted 27 October 2020
Available online 31 October 2020

Keywords:
Mixed rare earth oxide powder
Thorium
Bastnasite ore
Baking
Leaching
Precipitation

ABSTRACT

The production of mixed rare earth oxide powder from a thorium containing bastnasite ore by sulfuric acid bake-water leaching followed by precipitation with oxalic acid and thermal decomposition of the oxalates was investigated. The sulfuric acid baking was performed at 250 °C and the optimum baking time was found to be 3 h. Using deionized water as lixiviant, 92.6% La, 86.8% Ce, 86.9% Pr, 82.3% Nd, 95.4% Th and 31% Y were dissolved from the baked ore at 25 °C after 30 min of leaching. The effect of solid-to-liquid ratio on the dissolution of the rare earth elements and thorium shows that when the solid ratio in the water increased from 1:10 to 1:3, the dissolution percentage decreased. The final mixed rare earth oxide powder contained 88.54% REO and 6% ThO_2 together with small amounts of other impurities. The SEM mapping results revealed that the produced REO has an irregular crystal shape. Based on the experimental results obtained from the current study, a flowsheet was proposed for the production of mixed rare earth oxide powder from a specific complex bastnasite ore.

1. Introduction

The rare earth elements (REE) are critical raw materials for manufacturing many emerging electronics and advanced components with widespread fields of applications in the energy, medical, defense, aerospace and automotive industries [6,11,24,32]. The global consumption for REE was estimated between 120 and 150 kt in 2016 and the global demand for REE is expected to grow at an annual rate of 5% by 2020 [12]. This demand would continue to grow for a long time following the increasing growth of green and advanced technologies and thus, it is important to secure sustainable supply chains for REE to meet the growing demand.

The global production of REE is mainly derived from three mineral resources, namely bastnasite, monazite and xenotime [15,34]. Among these three, bastnasite (a fluorocarbonate mineral) is the most industrially important with its deposits in Bayan Obo, China, and Mountain Pass, USA, currently constitute the largest percentage of the world's rare earth resources. The processing of bastnasite ores at these two locations involves froth flotation processes to produce concentrates of rare earth oxides (REO) with an REO content of 50% or higher [20, 30, 31]. At Mountain Pass, these concentrates are further processed by caustic conversion in a supersaturated sodium hydroxide solution at 120–130 °C [23]. The produced rare earth hydroxides were then leached in hydrochloric acid solutions to dissolve the REE to allow the separation of the individual rare earth and precipitation of marketable compounds. Reportedly, only 10% of the bastnasite concentrates at Bayan Obo are processed by such a caustic conversion [51]. The rest of the concentrates are processed via a cheaper acid baking route in a 98% sulfuric acid solution at 400–500 °C [23,27,51]. This converted the fluorocarbonates to sulfates, which can be leached in water to dissolve the REE.

The formation of water-soluble sulfates of lanthanides ($Ln_2(SO_4)_3$) during the acid baking process occurs via Reaction (1). Thorium, if present, also forms soluble sulfate during baking. Gaseous carbon dioxide and hydrogen fluoride are released during the process but the latter can be captured as a by-product if the ore contains a high level of fluorite (CaF_2) and the baking is performed at a temperature higher than 200 °C [18] or recovered as solid ammonium fluoride (NH_4F) by reacting with ammonium carbonate ($(NH_4)_2CO_3$) [46]. The former reportedly provides natural agitation to the mixture and thus, mechanical agitation is not required when mixing the ore and sulfuric acid [35].

$$2LnFCO_3(s) + 3H_2SO_4(aq) = Ln_2(SO_4)_3(s) + 2HF(g) + 2CO_2(g) + 2H_2O(l) \quad (1)$$

Over the past two decades, the combination of pyro and hydrometallurgical method via acid roasting that is followed by leaching and

* Corresponding author.
E-mail address: sait.kursunoglu@agu.edu.tr (S. Kursunoglu).

https://doi.org/10.1016/j.powtec.2020.10.086
0032-5910/

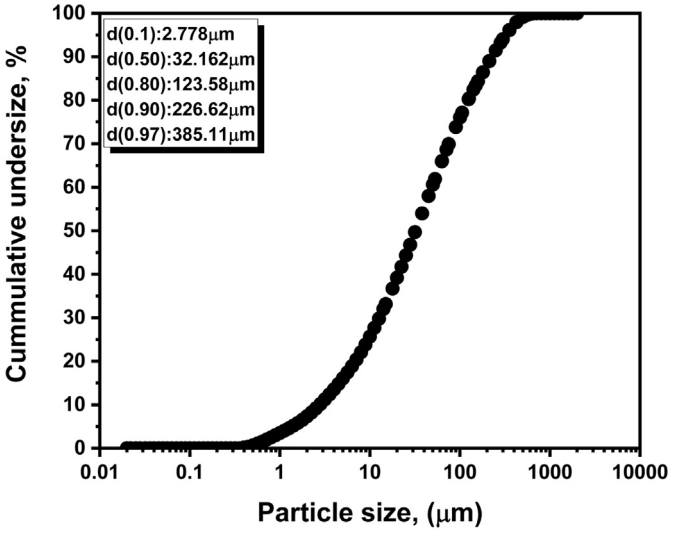

Fig. 1. The particle size distribution of the ground ore.

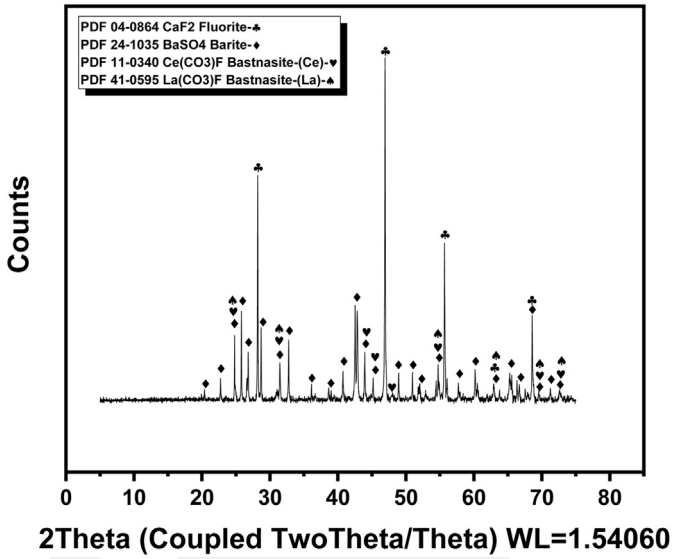

Fig. 2. X-ray diffraction pattern of the complex bastnasite ore.

precipitation has been the most common processing route for extracting REE not only from bastnasite but also monazite and xenotime [14,17,38,49]. In Malaysia, The Malaysian Rare Earth Corporation (MAREC) separated monazite and xenotime from the ores via magnetic separator to produce separate concentrates of each ore. The xenotime concentrate was converted to water-soluble sulfate by an acid bake process. The product was leached with cold water to produce yttrium-rich solution. Oxalic acid was then added to the pregnant leach solution to precipitate yttrium oxalate, which was subsequently calcined to produce yttrium oxides. The company produced 200 tons of yttrium concentrate, which comprised of 60% Y_2O_3 during the 1990s [39].

In Turkey, specifically at Beylikahir in the Eskisehir region, bastnasite occurs in complex ores consisting of high levels of fluorite and barite with thorium. The resource of such rare earth ores was estimated to be 1 million tons with an average grade of 3.14% REO [18,26]. The beneficiation of bastnasite from these ores is, however, difficult because these three minerals have similar specific gravity and floatability. The presence of high levels of fluorite is especially detrimental to the beneficiation process since complete fluorite flotation, to separate the mineral, would lead to high losses of bastnasite in the fluorite concentrate [4]. Moreover, the bastnasite mineral in these ores occurs either as cement material between fluorite and barite particles or is intimately associated with these two minerals [18].

Researchers have carried out attempts to beneficiate such a complex bastnasite ore. Ozbayoglu and Atalay [26] used attrition scrubbing followed by screening and desliming by cyclones to produce a so-called pre-concentrate containing about 23.5% REO. This pre-concentrate was then upgraded using a multi-gravity separator to produce an REO grade of 35.5%. The recovery of the proposed beneficiation process was, however, low at only about 48% relative to the original ore. Beneficiation via attrition scrubbing was also performed by Kul et al. [18] to produce a pre-concentrate with 23.5% REO content but the recovery was not reported. Our research groups have also attempted to beneficiate similar bastnasite ores using gravity separation and flotation techniques but satisfactory results cannot be attained. Therefore, in this study, we investigated the efficiency of the production of mixed REO powder from a complex bastnasite ore from Beylikahir, Turkey, as the object of research without prior physical beneficiation process. Also, we investigated the recovery of thorium together with the mixed REO product. We proposed the use of sulfuric acid baking-water leaching technique followed by oxalate precipitation to allow the dissolution [9,18] and precipitation [22,29,41] of thorium along with the REE. The proposed processing route to produce mixed rare earth oxide powder from such a complex ore without prior physical beneficiation has not been studied before. The results of this experimental study may help improve the resource utilization of complex bastnasite ores that contain high level of fluorite, barite and thorium.

Table 1
Elemental analysis of the complex bastnasite ore by XRF and ICP-MS.

Major elements[a] (>1%)		Minor Elements[a] (<1%)		Rare earths[b]		Radioactive elements[b]	
Element	Weight percentages (%)	Element	Weight percentages (%)	Element	ppm (mg/kg)	Element	ppm (mg/kg)
Ba	31.80	Pb	0.09	La	7248	Th	326.20
Ca	26.83	Zn	0.07	Ce	11,912	U	110.60
F	17.71	P	0.21	Y	291.30		
Fe	5.64	Sr	0.32	Pr	1052		
Si	4.05	Na	0.07	Nd	2683		
S	3.60	Nb	0.01	Sm	155.20		
Al	2.03	Mg	0.42	Eu	29.73		
Mn	1.44	Ti	0.20	Gd	83.65		
		Cl	0.01	Dy	44.61		
		K	0.76	Er	26.84		
				Yb	23.40		

[a] XRF analysis
[b] ICP-MS analysis

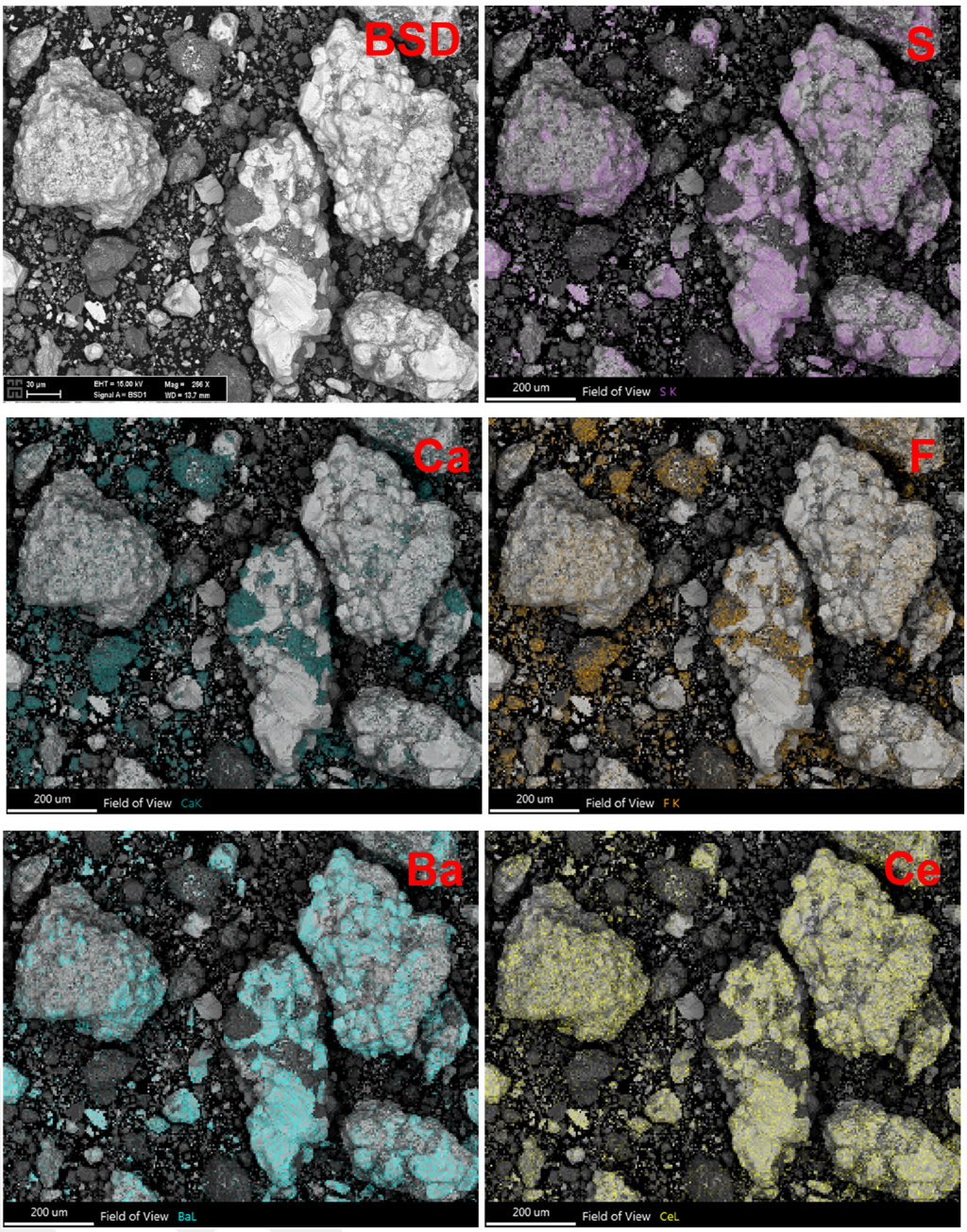

Fig. 3. SEM mapping of the complex bastnasite ore.

2. Material and methods

2.1. Material

The ore used in this study was provided by Eti Maden Operations General Directorate in Ankara, Turkey. The ore was firstly crushed in a laboratory jaw crusher and then ground in a laboratory ball mill. The milled ore was subjected to particle size analysis by using a laser diffraction particle analyzer (Malvern Mastersizer 2000). An X-ray fluorescence (XRF) spectrometer (Zetium, PANalytical and Axios Advance, PANalytical (for double-check)) was used for the elemental analysis of the ore. In addition, elemental analysis using inductively coupled plasma (ICP-MS, PerkinElmer-NexION 2000) was also performed to determine the REE content in the ore. The ore mineralogical composition was determined using an X-ray diffraction (XRD) instrument (Bruker Discover) at the Central Research Laboratory in Abdullah Gul University (AGU), which was calibrated with a silicon standard for alignment of the $2\theta = 5–75°$ or $2\theta = 10–80°$ using radiation generated at 40 mA and 40 kV. The mineral phases were identified using Diffrac Suite EVA software equipped with the current ICDD PDF-2/Minerals database. A field emission scanning electron microscopy (FE-SEM) coupled with energy-dispersive X-ray spectroscopy (EDX) (Zeiss GeminiSEM 300) was used for ore characterization at the AGU's Central Research Laboratory.

2.2. Methods

2.2.1. Sulfuric acid baking

In the sulfuric acid baking experiments, 50 g of ore and 50 g of analytical grade sulfuric acid (98% purity of H_2SO_4, Merck) were weighted and transferred into a 500-mL glass beaker. The slurry was stirred manually using a stirring rod to allow diffusion of acid to the ore sample and subsequently, the beaker was placed on a temperature-controlled

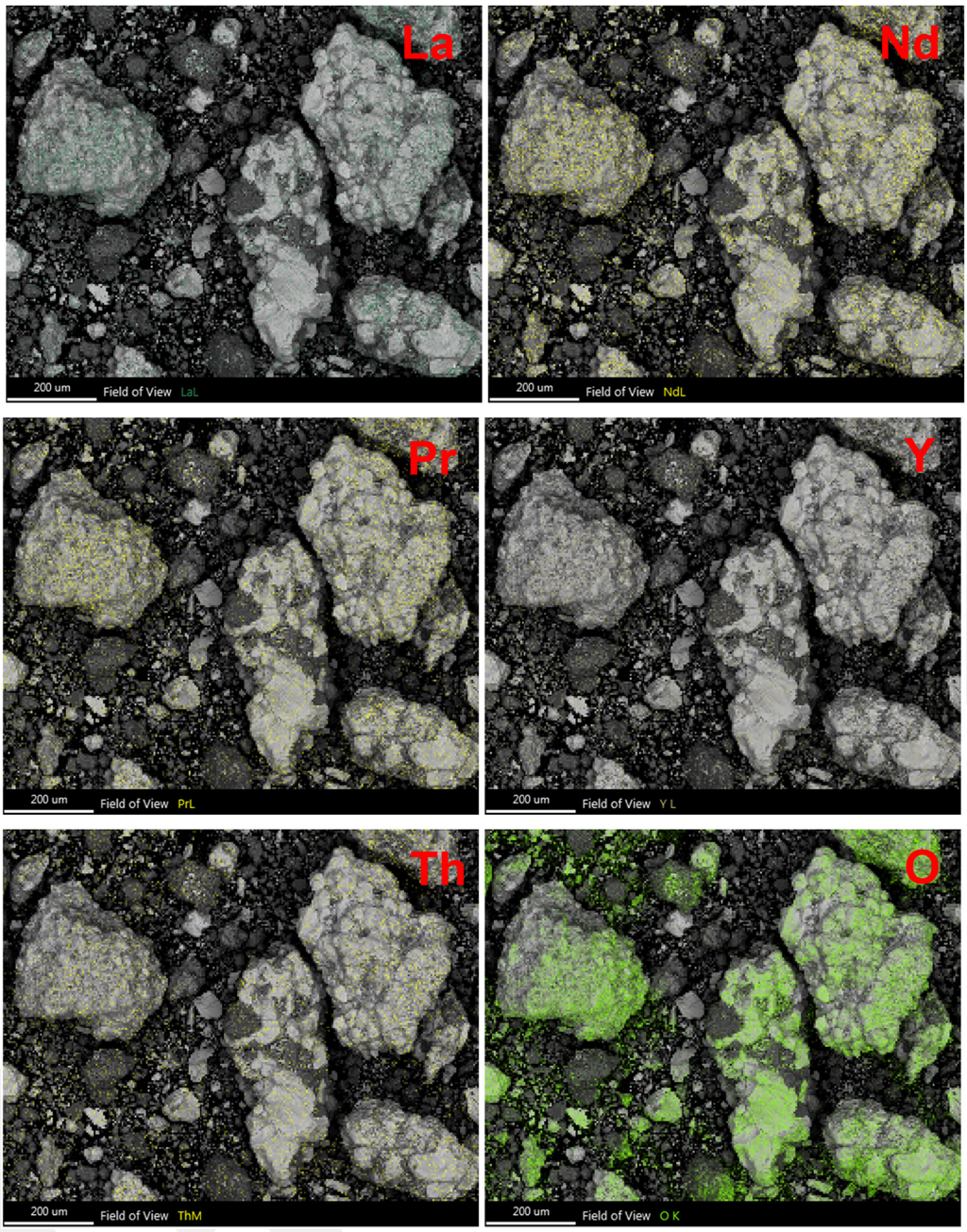

Fig. 3 (*continued*).

ceramic hot plate at 250 °C. After a certain baking duration, the beaker was removed from the hot plate and allowed to cool down before the baked ore was gently stripped from the beaker. The stripped sample was then transferred into an oven at 100 °C for 3 days. The dried sample was then digested and analyzed by ICP-MS. The solid-to-liquid (S/L) ratio was chosen to be 1:1 (*w*/w) in all the baking experiments. The baking experiments were carried out for 1 to 3 h.

2.2.2. Water leaching

The water leaching experiments were carried out by transferring 20 g of the baked sample into a 250-mL round-bottom glass flask after adding 200 mL of deionized water. Unless otherwise stated, the S/L ratio of 1:10 (*w*/*v*) was kept constant in all experiments. The agitation of the sample was provided by a digital magnetic stirrer equipped with a temperature-controlled heating mantle (MTOPS-MSDSM). The temperature and stirring speed were kept at 25 °C and 400 rpm, respectively, in all leaching experiments, while the duration of the stirring was varied between 30 and 90 min. After the leaching experiment was finished, the slurry was filtered with Whatman 1 filter paper. The obtained filtrates were then analyzed by ICP-MS. The dissolution percentage was determined using the following equation:

$$Dissolution(\%) = \frac{c_l \times V_L}{c_s \times M_S} \times 100\% \quad (2)$$

where, c_l is the REE concentration in the leachate (mg/L), V_L the volume of the analyzed leachate (L), c_s the REE concentration in the baked ore sample (mg/kg), and M_S the weight of the baked ore sample (kg).

2.2.3. Precipitation

The precipitation experiments used the pregnant leach solutions (PLS) collected from the acid bake-water leaching experiments under the determined optimum conditions. The pH of the PLS was measured

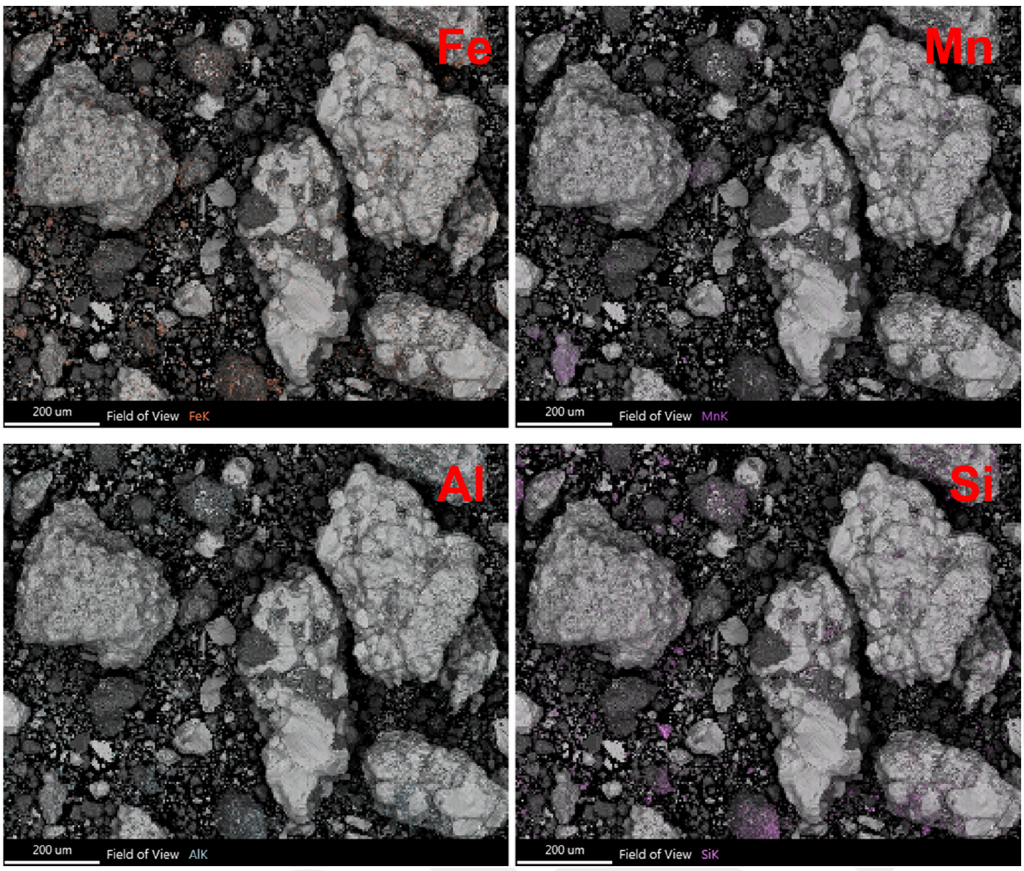

Fig. 3 (*continued*).

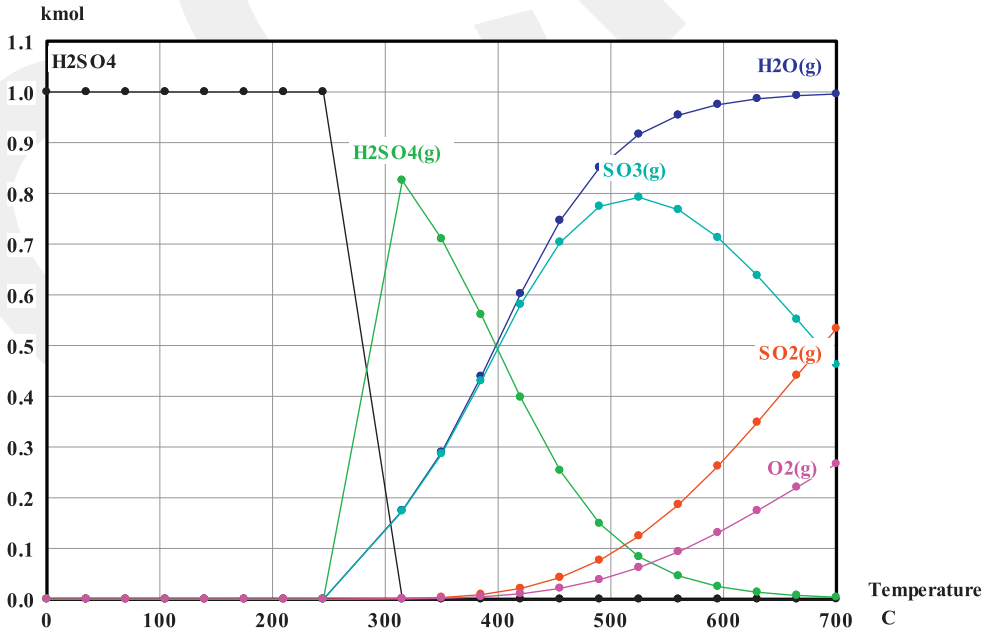

Fig. 4. Equilibrium composition of sulfuric acid as a function of temperature (1 kmol sulfuric acid, total pressure: 1 bar, HSC Chemistry 6).

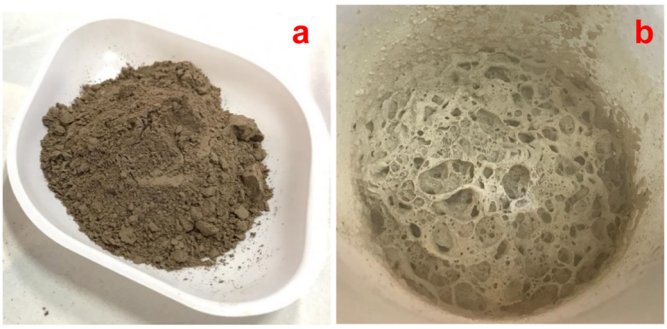

Fig. 5. a) Original ore sample, b) Sulfuric acid baked ore sample at 250 °C for 3 h.

by pH meter (Hach HQ40d) equipped with IntelliCAL PHC 28101 probe. The precipitating agent was 0.5 mol/L oxalic acid, which was freshly prepared from analytical grade oxalic acid ($H_2C_2O_4.2H_2O$, Merck) and deionized water. The reaction of the lanthanides (Ln^{3+}) with oxalic acid can be expressed as:

$$2Ln^{3+}(aq) + 3H_2C_2O_4 + nH_2O = Ln_2(C_2O_4)_3.nH_2O\downarrow + 6H^+(aq) \quad (3)$$

The experiment was performed using 100 mL of the PLS in a glass beaker heated on a temperature-controlled hot plate equipped with magnetic stirred. To avoid excessive evaporation, the glass beaker was covered with aluminum foil during the experiment. Once the desired temperature reached, the precipitating agent was delivered slowly using a syringe with a needle while the solution is stirred at a speed of 200 rpm. The period of the precipitating agent addition was 30 min, followed by 60 min of aging time at the same temperature and stirring speed. Subsequently, the slurry was allowed to settle at ambient temperature for 24 h. The precipitate was then filtered through Whatman 42 filter paper. The solid was collected and oven-dried at 100 °C for 1 h, while the filtrate was collected for ICP-MS analysis. The precipitation percentage of the REE as a function of temperature was calculated based on the difference of the REE concentration in the solution before and after the precipitation experiment, expressed as:

$$Precipitation(\%) = \frac{c_i \times V_i - c_f \times V_f}{c_i \times V_i} \times 100\% \quad (4)$$

where, c_i is the initial REE concentration in the PLS (mg/L), c_f the final REE concentration in the PLS (mg/L), V_i the initial volume of the PLS (L) and V_f the final volume of the PLS (L).

Table 2
Results of elemental analysis of the baked ore at 250 °C for different times.

Element	250 °C 1 h acid baking ppm (mg/kg)	250 °C 2 h acid baking ppm (mg/kg)	250 °C 3 h acid baking ppm (mg/kg)
La	5096	5187	5094
Ce	8018	8178	8049
Y	199.60	200.40	198.10
Pr	725.60	740.40	732.90
Nd	1838	1849	1826
Sm	104.50	104.70	104
Eu	19.60	19.60	19.60
Gd	56.40	56.60	56.30
Dy	29.50	29.70	29.40
Er	17.90	17.90	17.90
Yb	15.30	15.50	15.30
Th	738.70	741.40	739.70
U	62.60	62.80	62.70

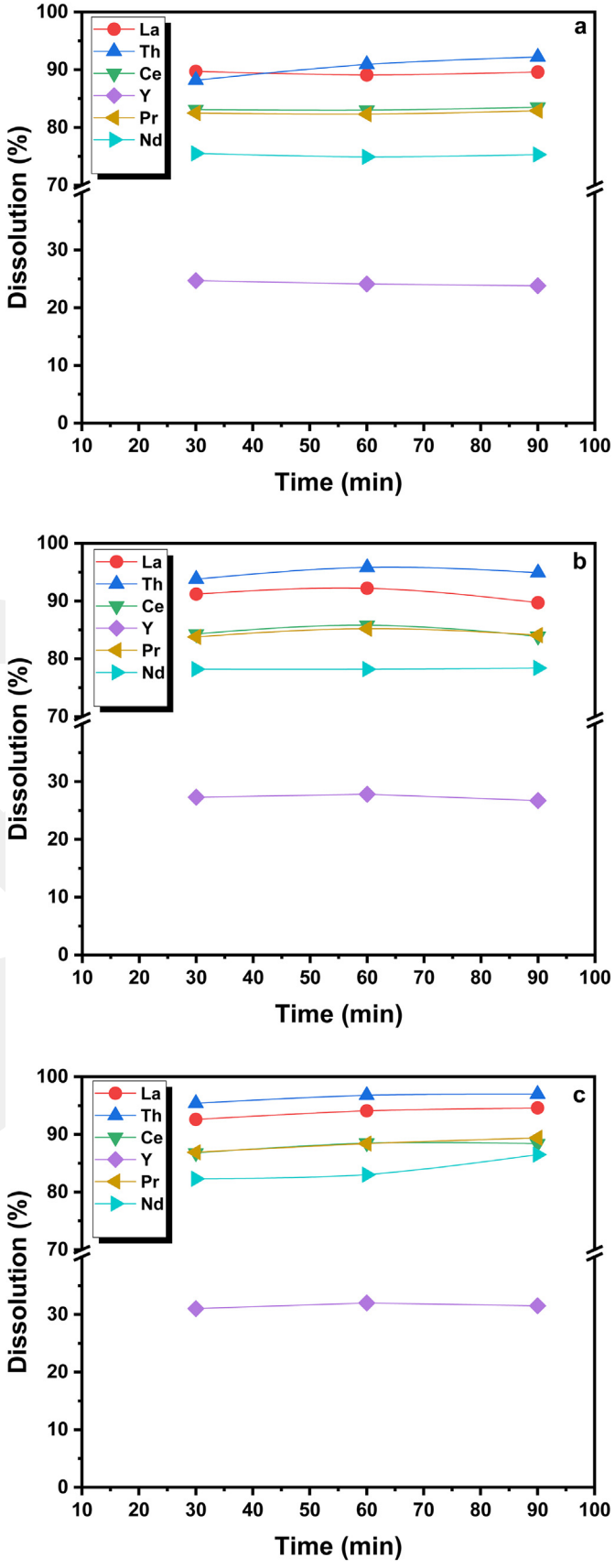

Fig. 6. Effect of leaching time on the dissolution of rare earth elements and thorium from baked ores at 25 °C (a- baked ore at 250 °C for 1 h, b- baked ore at 250 °C for 2 h, c- baked ore at 250 °C for 3 h).

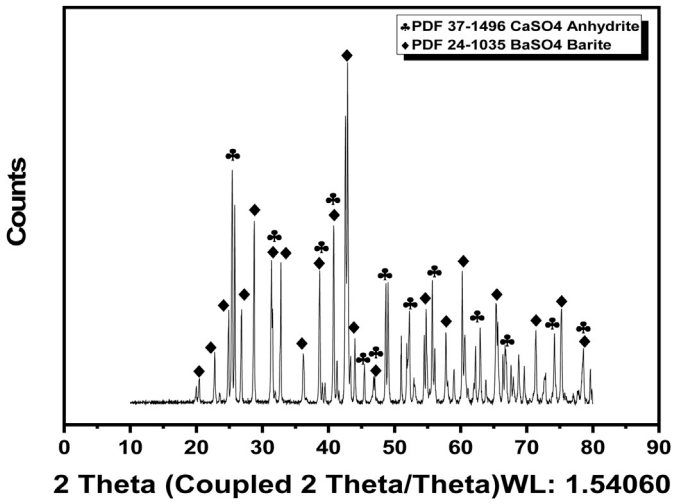

Fig. 7. XRD pattern of the baked ore after leaching with water (250 °C acid baking for 3 h, solid to liquid ratio of 1:10, leaching with water at 25 °C for 30 min).

2.2.4. Thermal decomposition

The thermal decomposition of the obtained rare earth oxalates was carried out in a muffle furnace (Lenton Thermal Furnace). The solid sample, obtained from the optimum precipitation test condition, was placed on a porcelain crucible (Ø 30 mm/38 mm) and heated in the furnace at 900 °C for 2 h. The decomposed sample was then subjected to XRD analyses to verify the transformation of the rare earth oxalates to rare earth oxides. The sample was then analyzed by XRF to determine the chemical composition of the rare earth oxides. SEM analyses were also performed to reveal the morphological structure of the mixed rare earth oxides. The thermal decomposition reactions can be expressed as followings:

$$Ln_2(C_2O_4)_3.nH_2O = Ln_2(C_2O_4)_3 + nH_2O\uparrow \quad (5)$$

$$Ln_2(C_2O_4)_3 = Ln_2(C_2O_4)(CO_3)_2 + 2CO\uparrow \quad (6)$$

$$Ln_2(C_2O_4)(CO_3)_2 = Ln_2(CO_3)_3 + CO\uparrow \quad (7)$$

Table 3
The mean concentration of PLS collected from the optimum conditions (pH: 0.80).

Element	mg/L	Rare Earth Element	mg/L	Radioactive Element	mg/L
Al	206.80	La	486	Th	73.35
As	16.80	Ce	718	U	7.24
Ba	0.48	Y	5.26		
Ca	676.30	Pr	64.27		
Cu	1.51	Nd	149.20		
Fe	799.30	Sm	6.15		
K	333.50	Eu	0.96		
Mg	63.13	Gd	3.10		
Mn	55.12	Dy	0.92		
Mo	3.27	Er	0.52		
Na	78.69	Yb	0.50		
Nb	2.96	∑REE	1434.80		
P	45.57				
Pb	1.71				
S	1813				
Ti	29.95				
Zn	14.14				

$$Ln_2(CO_3)_3 = Ln_2O(CO_3)_2 + CO_2\uparrow \quad (8)$$

$$Ln_2O(CO_3)_2 = Ln_2O_2CO_3 + CO_2\uparrow \quad (9)$$

$$Ln_2O_2CO_3 = Ln_2O_3 + CO_2\uparrow \quad (10)$$

3. Results and discussions

3.1. Material characterization

The size distribution, chemical and mineral composition of the sample was analyzed. The particle size distribution of the ground sample is shown in Fig. 1. The results showed that 80% of the sample was smaller than 124 μm. Table 1 shows the chemical compositions of the sample by the XRF analysis. The REE concentrations obtained from the ICP analysis are also included in Table 1. The XRD patterns of the sample depicted in Fig. 2 show that the major peaks were from fluorite (card no: 04–0864) and barite (card no: 24–1035). The minor peaks were determined as Ce-bastnasite (card no: 11–0340) and La-bastnasite (card no: 41–0595). The presence of high levels of fluorite and barite in the sample is in agreement with the findings of Yorukoglu et al. [47], Kul et al. [18] and Kursun et al. [19] who also used bastnasite ores from the Eskisehir

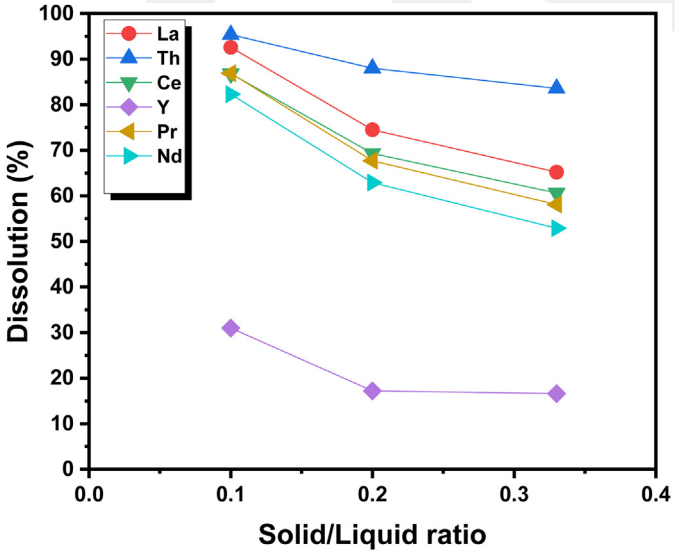

Fig. 8. Effect of solid to liquid ratio on the dissolution of rare earth elements and thorium from the 250 °C baked ore for 3 h, leaching with water at 25 °C for 30 min.

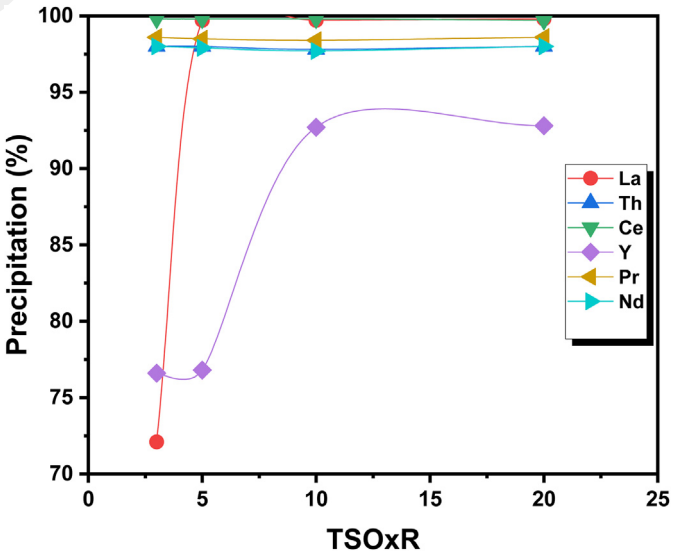

Fig. 9. Precipitation percentage of the REE and thorium from the PLS using different stoichiometric times of oxalic acid at 75 °C.

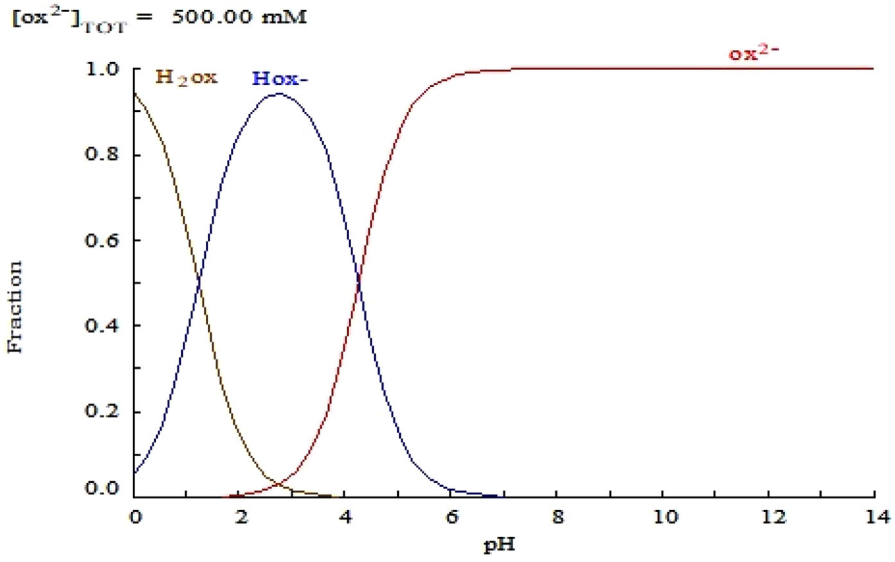

Fig. 10. The distribution of three species of oxalic acid at a concentration of 0.5 mol/L (Software Medusa-ChemicalEquilibrium Diagram).

region. Representative SEM mapping results of the sample are shown in Fig. 3. The SEM results revealed that the major constituents of the ore were calcium, fluorine, barium and iron-containing minerals. The results also indicate that most of the REE occurred either as cement material between fluorine and barium particles or were intimately associated with these elements.

3.2. Effect of baking and leaching time on dissolution

Previous studies show that baking temperatures of higher than 200 °C are required to achieve complete decomposition of bastnasite and monazite concentrates within reasonable baking time to allow high dissolutions of the REE [8,35,37,40]. The equilibrium composition of sulfuric acid as a function of temperature simulated using HSC Chemistry version 6, shown in Fig. 4, however, indicates that the acid is started to decompose at ~200 °C. Therefore, while increases in baking temperature up to 330 °C enhances the leaching efficiencies of the REE in bastnasite and monazite, the use of lower baking temperatures is more desirable to not only save energy cost but also minimize evaporative loss of the acid [8]. In agreement with the computed equilibria, Soltani et al. [37] experimentally found that decomposition of sulfuric acid is negligible at temperatures of 200–250 °C. Hence, in this study, the baking experiments were performed at 250 °C at various baking durations ranging between 1 and 3 h. Baking at these temperatures showed that almost complete solubilization of the rare earth elements and thorium was achieved in the subsequent water leaching. Schwartz et al., [34], Li et al., [21], Wang et al., [43] and Demol et al., [8] were indicated that bake duration varies between 0.5 h and 4 h for monazite bearing concentrate whereas baking temperatures were achieved at greater than 200 °C for complete decomposition [36,40].

The evolutions of gases from the baking reactions are apparent from the spongy feature of the baked sample (Fig. 5 b). The fluorite (CaF_2) in the ore is transformed into one of either gypsum ($CaSO_4.2H_2O$), hemihydrate ($CaSO_4.0.5H_2O$), or anhydrite ($CaSO_4$) during the sulfuric acid baking experiments [18,37]. The elemental concentrations of the samples baked for 1, 2 and 3 h are depicted in Table 2. The water leaching tests on these baked samples were then carried out for up to 90 min at 25 °C. Notably, the effect of leaching temperature on the leaching efficiency was not studied [25] since the solubility of lanthanide sulfates in water decreases with an increase in temperature owing to the exothermic nature of their dissolutions in water [18,48].

The leaching results, depicted in Fig. 6, show that the dissolutions of the REE and Th from the three baked samples were relatively constant throughout the tested leaching duration suggesting that the dissolution reactions occurred rapidly. Chemical analyses of the PLS obtained from the sample baked for 1 h showed that 89.7% La, 83.1% Ce, 82.5% Pr and 75.5% Nd were dissolved from the sample along with 85% of Th after 30 min of leaching, while Y dissolution was only 24.7% (Fig. 6a). The dissolutions of La, Ce, Pr, Nd, Y and Th were increased to 92.6%, 85.8%, 85.9%, 82.3%, 31%, and 95.4%, respectively, after 30 min of leaching when the baking duration was increased to 3 h (Fig. 6c).

Fig. 7 shows the XRD patterns of the sample baked at 250 °C for 3 h followed by water leaching at 25 °C for 30 min. The patterns revealed that the major peaks originate from barite (card no: 24–1035) and calcium sulfate anhydrite (card no: 37–1496). These show that fluorite was mainly transformed into anhydrite and that the formed anhydrite was poorly soluble in water and its recrystallization to gypsum after leaching was minimal. These are consistent with the findings of Kul

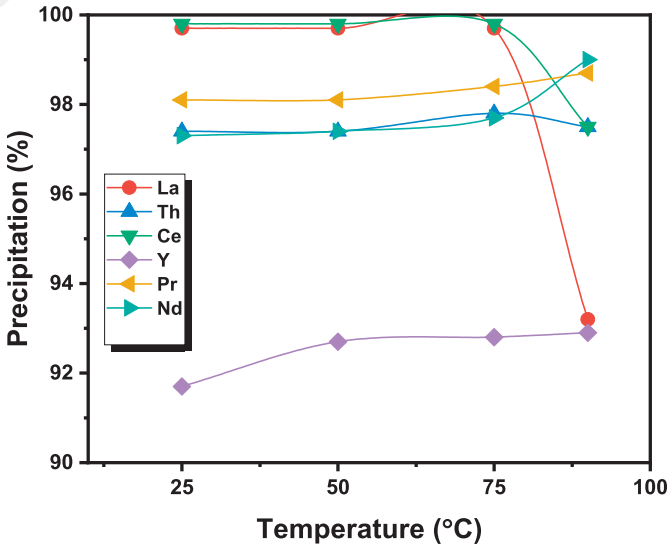

Fig. 11. Precipitation percentage of REE and thorium from the PLS using 10 TSOxR at different temperatures.

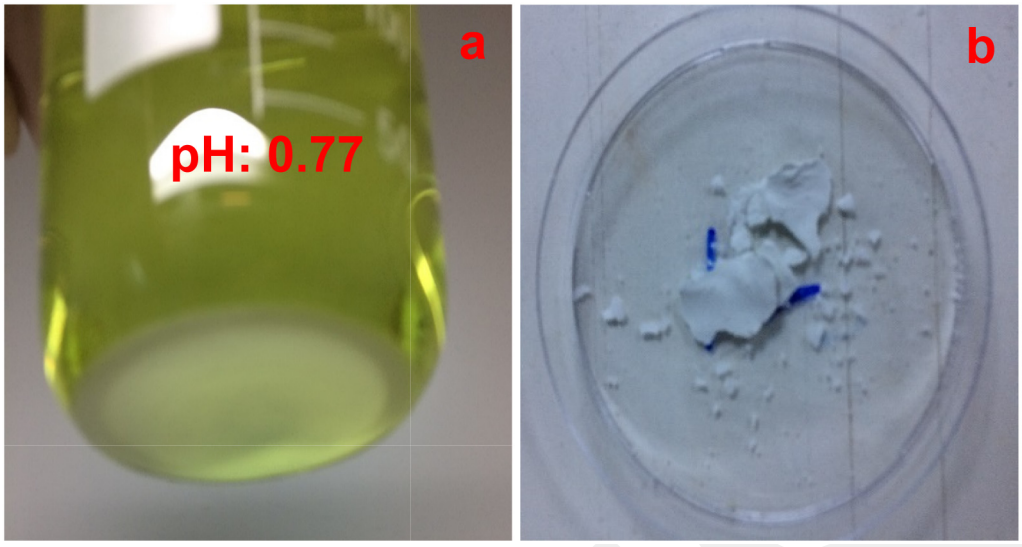

Fig. 12. a) Precipitated rare earth oxalates from the leach solution using 10 TSOxR at 25 °C, b) Produced rare earth oxalate powder after drying.

et al. [18] and Soltani et al. [37] with bastnasite and monazite concentrates, respectively.

3.3. Effect of solid-to-liquid ratio on dissolution

The effect of solid-to-liquid ratio ranging from 1:10 to 1:3 (*w*/*v*) on the dissolutions of REE and Th from the baked sample obtained at 250 °C after 3 h baking time was studied at a leaching temperature of 25 °C. The results, depicted in Fig. 8, show that the dissolution percentage of the REE markedly decreased when the solid-to-liquid ratio during leaching was increased from 1:10 to 1:3. This can be attributed to the relative decrease in the amount of solvent per unit of solid at the higher solid-to-liquid ratios, which appears to lowered the solubility of the metals since their dissolutions were observed to be relatively unchanged after 30 min of leaching. Given these results, the solid-to-liquid ratio of 1:10 was determined to be optimum. Kul et al., [18] studied the effect of solid-liquid ratio on the dissolution of rare earth elements from pre-concentrate ore. They stated that when the solid-to-liquid ratio was changed from 1:8 to 1:3, the rare earth concentrations remained constant. Barghusen and Smutz, [2], Vijayalakshmi et al., [42] and Kim and Osseo-Asare, [16] reported that an optimum solid-to-liquid ratio was varied between 1:4–1:10 for the dissolution of rare earth elements from high-grade mineral concentrates.

3.4. Precipitation of leach solution with oxalic acid

The precipitation tests were carried out using the PLS obtained from leaching the sample that was baked at 250 °C for 3 h in the water at a solid-to-liquid ratio of 1:10 and a temperature of 25 °C for 30 min. The mean concentration of the produced PLS is given in Table 3. The average pH of the PLS was 0.80. The measured low pH is due to the remaining acid left after baking. The precipitating agent used was oxalic acid, which is known to have a strong affinity toward trivalent REE ions to form REE oxalates that have low solubility in aqueous solution [3]. The oxalic acid addition was calculated as the times of stoichiometric oxalic acid requirement (TSOxR) for the total molar concentration of REE ions in the PLS ($\sum$REE) to precipitate as oxalates. The concentrations of other elements were not been taken into consideration for the calculation of the oxalic acid requirement. It is known that the produced mixed rare earth oxalates contain a substantial amount of Th and can lead to contamination in the mixed rare earth oxalates [5,28]. However, the addition of reagent for the removal of impurities before oxalate precipitation can create some drawbacks such as complexity of recovery, opex, capex and environmental impact.

Precipitation temperature has an important effect on oxalate activity, solubility and metal complex stability. The precipitation of REE was initially conducted at 75 °C to allow better crystallization (Fig. 9). It can be seen that more than 95% of Ce, Nd, Pr and Th were precipitated at 3 TSOxR, while La and Y precipitations were below 77%. The results indicate that Ce, Nd, Pr and Th precipitations become more favorable than La and Y precipitations at lower TSOxR. The precipitation of La increased sharply when the oxalic acid addition was 5 TSOxR but the Y precipitation almost remained constant. A possible reason for this tendency is that the yttrium oxalate has a high solubility at higher pHs [45]. The maximum simultaneous REE precipitation was achieved when the oxalic acid addition was 10 TSOxR. No further increases in the precipitation percentage were observed when the oxalic acid addition was increased up to 20 TSOxR. The results obtained from the precipitation experiments were consistent with the findings of [1]. The

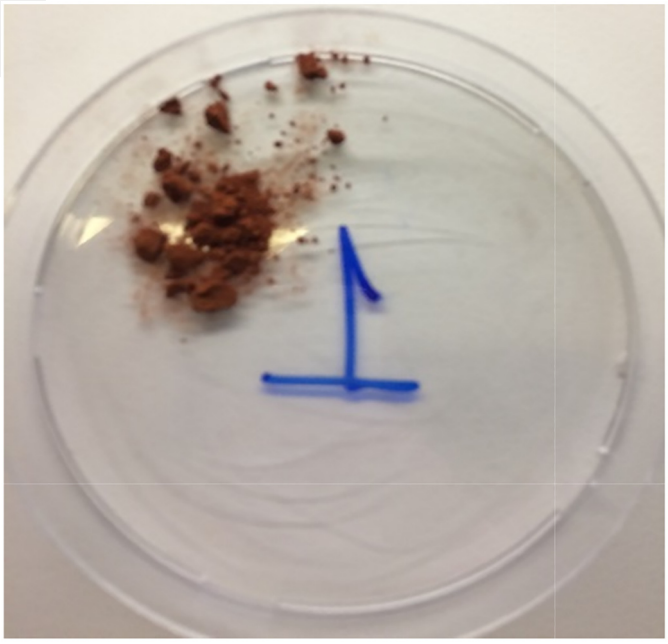

Fig. 13. Produced mixed rare earth oxide powder after thermal decomposition.

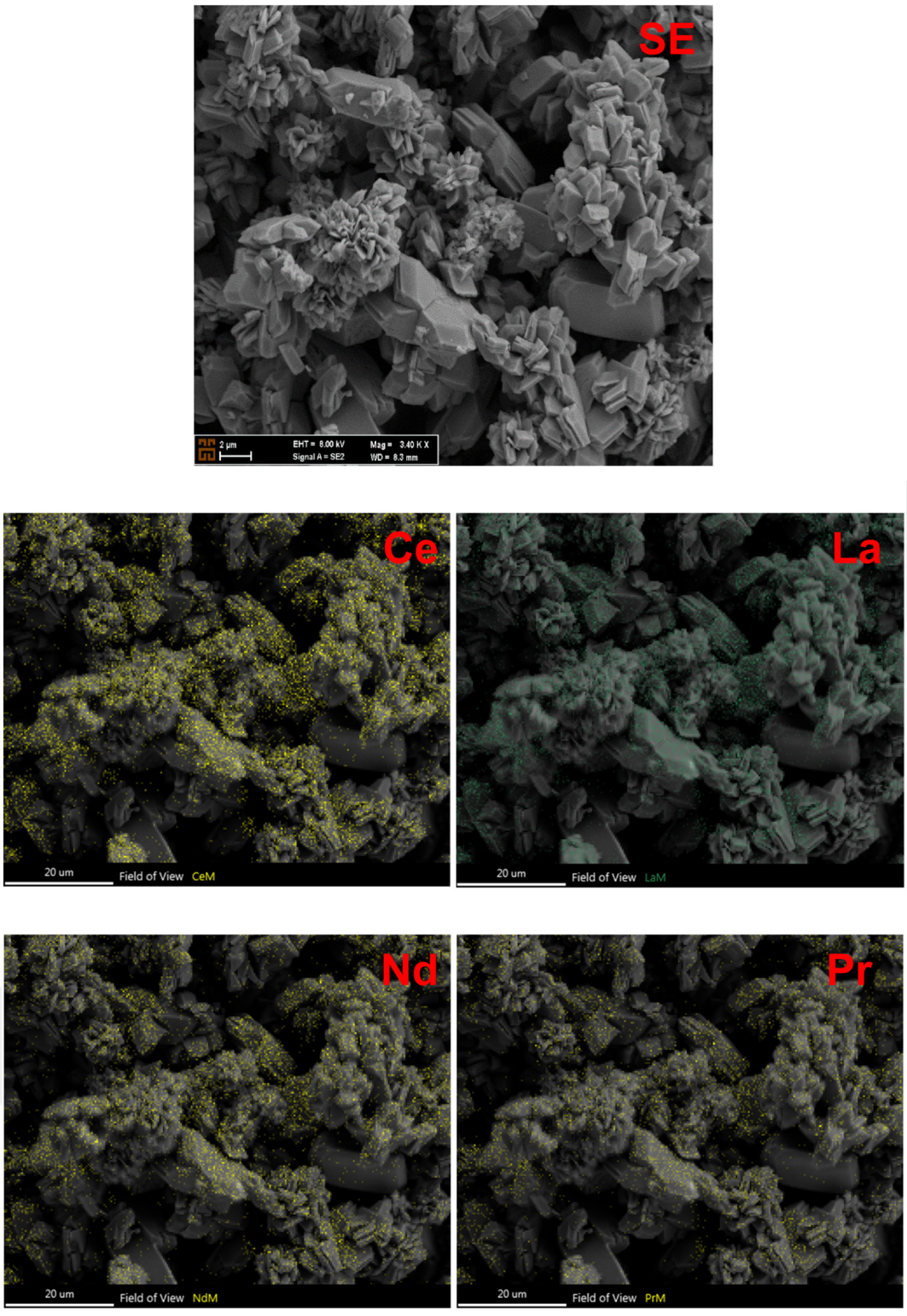

Fig. 14. SEM mapping of the produced mixed rare earth oxide powder.

authors reported that 10 times the stoichiometric amount of oxalic acid was required for the precipitation of REE from their PLS.

The solution pH is an important factor for an oxalate precipitation process as the pH is affecting the activity of the dissociated oxalate anions. The speciation diagram of oxalic acid shown in Fig. 10 for an acid concentration of 0.5 mol/L, wherein $HC_2O_4^-$ and $C_2O_4^{2-}$ ions are the predominant species in the pH ranges of 2.5–3 and 7–14, respectively, explain why the reaction rate increases over these pH ranges. Theoretically, therefore, the total oxalic acid requirement decreases and the metal recovery increases with increasing pH owing to the higher oxalate ionization. Increasing the pH, however, also lead to lower product purity owing to co-precipitation of impurities such as iron and

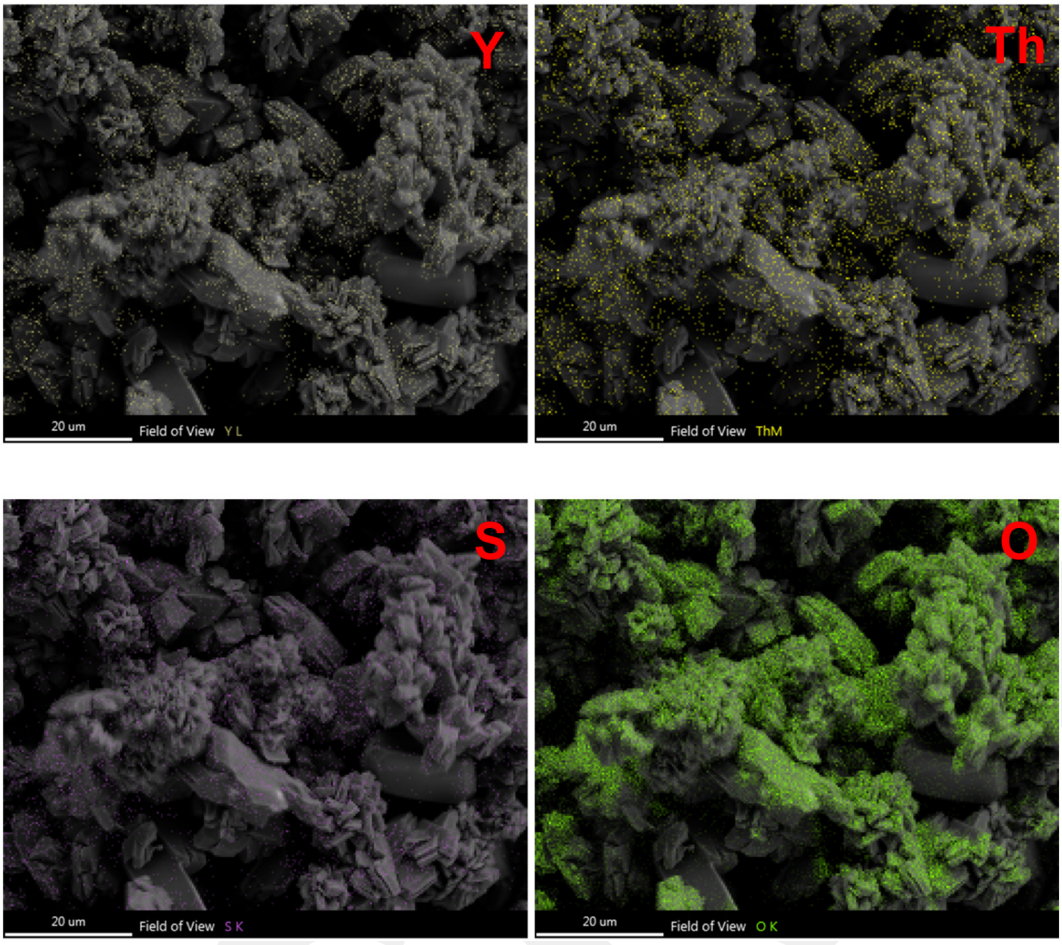

Fig. 14 (*continued*).

aluminum as has been experimentally shown by Chi and Xu [7]. These authors found that the REE precipitation increased significantly when the pH increased from ~0 to 0.5, wherein it reached a plateau and increased only slightly with further increases in pH. These findings are in agreement with this study, wherein more than 97% of the REE and Th, except Y, were precipitated from the PLS, which had a pH of 0.8, without any pH adjustment. Based on these, the effect of pH on the precipitation recovery was not pursued in this study.

The effect of temperatures ranging from 25 to 90 °C on the precipitation of REE and Th using 10 TSOxR is shown in Fig. 11. At 25 °C, 99.7% La, 99.8% Ce, 97.3% Nd, 98.1% Pr, 91.7% Y and 97.4% Th were precipitated from the solution. The precipitation percentage of these metals were relatively unchanged when the temperature was increased from 25 to 75 °C. When the precipitation temperature was increased further to 90 °C, the La and Ce precipitation percentages decreased significantly to 93.2% and 97.5%, respectively. It can be attributed to the fact that the oxalate precipitation at elevated temperatures appeared to fit into the tendency observed in double-sulfate salt precipitation where the solubility of the double-sulfate salt decreases with the increasing precipitation temperature. Given the fact that increasing temperature does not affect the precipitation recovery significantly, 25 °C was determined to be the optimum precipitation temperature in this study. Images of the precipitated oxalates from the leach solution using 10 TSOxR at 25 °C is shown in Fig. 12. The pH of the barren leach solution (BLS) was measured to be 0.77 (Fig. 12a), which was precipitated as rare earth oxalates from the leach solution using 10 TSOxR at 25 °C. Fig. 12b shows the produced rare earth oxalate powder after drying.

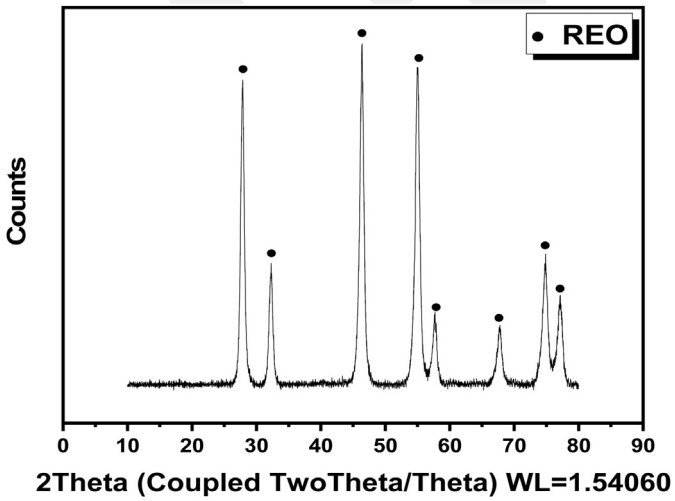

Fig. 15. The pattern of produced mixed rare earth oxide powder.

3.5. Thermal decomposition of precipitate

The last step in this research is the thermal decomposition of the obtained rare earth oxalate powder. The mixed rare earth oxalate powder

Table 4
The chemical composition of the mixed rare earth oxide powder by XRF.

Compound	Weight percentages (%)
*CeO_2	44
*La_2O_3	27
*Nd_2O_3	12
*Pr_2O_3	4.70
*Y_2O_3	0.84
ThO_2	6
SO_3	2.10
Cs_2O	0.90
CaO	0.84
Nb_2O_5	0.33
TiO_2	0.26
SiO_2	0.25
P_2O_5	0.24
Fe_2O_3	0.15
Al_2O_3	0.14
CuO	0.13
PdO	0.12
*∑REO	88.54

produced under the optimum precipitation conditions were roasted in a muffle furnace at 900 °C for 2 h to convert them to rare earth oxide powder (REO). Fig. 13 shows the produced mixed rare earth oxide powder. The produced mixed REO powder were investigated by SEM mapping method (Fig. 14). The product has an irregular crystal shape. Fig. 15 shows the XRD patterns of the produced mixed REO powder. The results show eight REO powder peaks that are consistent with the findings of Zhu et al., [50] for Nd_2O_3, Dy_2O_3 and Eu_2O_3; Djenadic et al., [10] for REO containing Ce, La, Sm, Nd, Pr, and Y, Gomes et al., [13] for REO containing Er, Dy, Y, and Yb, and Wang et al., [44] for CeO_2. The diffraction peaks of the mixed rare earth oxide powder are also sharp without any impurity peaks, indicating that the purity of the product was high. The chemical composition of the produced material at 900 °C for 2 h is given in Table 4. The total REO powder concentration was found to be 88.54%. The concentration of ThO_2 was found to be 6%, and 0.84% CaO, 0.15% Fe_2O_3, 0.14% Al_2O_3 and 0.13% CuO was detected in the product.

3.6. Proposed flowsheet

Fig. 16 demonstrates the proposed flowsheet for the production of mixed rare earth oxide powder from the thorium containing bastnasite ore. The sulfuric acid baking produces HF gas, which can be converted to solid NH_4F by reacting with $(NH_4)_2CO_3$ [46]. The water-soluble sulfates of lanthanides and Th were dissolved into the PLS while $CaSO_4$ and $BaSO_4$ remained in the leach residue, which can be selectively recovered by the conventional mineral processing techniques. The produced PLS at optimum conditions were subjected to a precipitation process with oxalic acid. It was determined that there is no selective precipitation in this stage as the REE is precipitated along with Th at all the tested experimental conditions. In the last stage, thermal decomposition was conducted at 900 °C for 2 h to convert the produced rare earth oxalate powder to oxides. The final product containing 88.54% REO and 6% ThO_2 was produced together with other impurities such as iron, aluminum, copper and calcium. Based on these experimental results, a flowsheet was proposed.

4. Conclusions

Sulfuric acid bake-water leaching, precipitation with oxalic acid followed by thermal decomposition on the thorium containing bastnasite ore was investigated for the production of mixed rare earth oxide powder. The best sulfuric acid baking temperature was

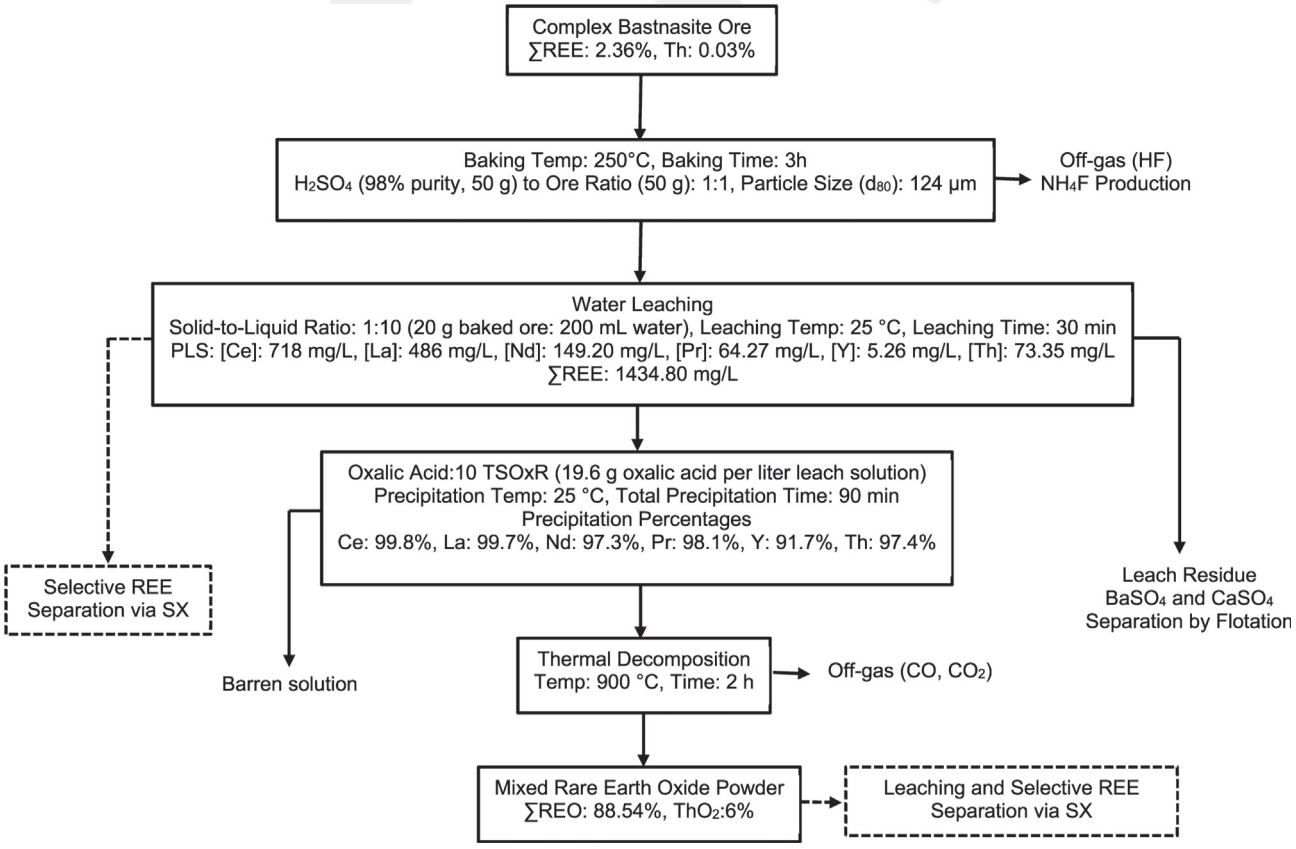

Fig. 16. Proposed flow sheet for the production of mixed rare earth oxide powder from the thorium containing bastnasite ore (dashed lines indicate future works).

determined to be 250 °C, and the optimum baking time was found to be 3 h. The optimum water leaching conditions were found to be the following: leaching temperature of 25 °C, a solid-to-liquid ratio of 1:10, and leaching time of 30 min. Under these conditions, 86.8% Ce, 92.6% La, 86.9% Pr, 82.3% Nd, 95.4% Th and 31% Y were extracted from the baked sample. The optimum conditions for the production of mixed rare earth oxalates from the produced PLS were the following: precipitation temperature of 25 °C, precipitation time of 90 min, and oxalic addition of 10 times the stoichiometric amount of the REE and Th presence in the baked ore. Under these conditions, 99.8% Ce, 99.7% La, 97.3% Nd, 98.1% Pr, 91.7% Y and 97.4% Th were precipitated from the PLS. Subsequently, the produced oxalates were roasted in a muffle furnace to convert the mixed rare earth oxalate powder to oxides at 900 °C for 2 h. The converted product contained 88.54% REO and 6% ThO_2 along with small amounts of other impurities such as 0.84% CaO, 0.15% Fe_2O_3, 0.14% Al_2O_3 and 0.13% CuO. The XRD confirms that the produced mixed rare earth oxide powder are consistent with the findings of previous researchers. The SEM mapping results on the produced mixed REO powder revealed an irregular crystal shape structure product, which contains a considerable amount of rare earth elements and thorium. As a result, mixed REO powder were produced from the thorium containing complex bastnasite ore. Based on the experimental results, a flowsheet was proposed. The separation and purification of thorium and rare earth elements from the produced PLS and the mixed REO powder by leaching and solvent extraction (SX) is currently under investigation by our research group.

Declaration of Competing Interest

The authors declare that they have no known competing financial interests or personal relationships that could have appeared to influence the work reported in this paper.

Acknowledgements

The authors are grateful to Tuncay Bircan from Eti Maden Operations General Directorate for providing the ore sample. The corresponding author thanks A. F. Yazici from Abdullah Gul University, Department of Materials Science and Nanotechnology Engineering for the SEM analysis.

References

[1] Anvia, M., Ho, E., Soldenhoff, K. 2013. Alternative process for rare earth recovery frombastnasite containing ore. COM hosted by MS&T13.
[2] J. Barghusen, M. Smutz, Processing of monazite sands, Ind. Eng. Chem. 50 (1958) 1754–1755.
[3] D. Beltrami, G. Cote, H. Mokhtari, B. Courtaud, B.A. Moyer, A. Chagnes, Recovery of uranium from wet phosphoric acid by solvent extraction processes, Chem. Rev. 114 (24) (2014) 12002–12023.
[4] S.M. Bulatovic, Flotation of REO Minerals, Handbook of Flotation Reagents: Chemistry, Theory and Practice: Flotation of Gold, PGM and Oxide Minerals, Elsevier Science, Amsterdam, 2010 151–173.
[5] R.J. Callow, The Industrial Chemistry of the Lanthanons, Yttrium, Thorium and Uranium, Pergamon Press, 1967.
[6] Z. Chen, Z. Zhang, D. Liu, X. Chi, W. Chen, R. Chi, Swelling of clay minerals during the leaching process of weathered crustelution-deposited rare earth ores by magnesium salts, Powder Technol. 367 (2020) 889–900.
[7] R. Chi, Z. Xu, A solution chemistry approach to the study of rare earth element precipitation by oxalic acid, Metall. Mater. Trans. B 30 (1998) 189–195.
[8] J. Demol, E. Ho, G. Senanayake, Sulfuric acid baking and leaching of rare earth elements, thorium and phosphate from a monazite concentrate: effect of bake temperature from 200 to 800 °C, Hydrometallurgy 179 (2018) 254–267.
[9] J. Demol, E. Ho, K. Soldenhoff, G. Senanayake, The sulfuric acid bake and leach route for processing of rare earth ores and concentrates: a review, Hydrometallurgy 188 (2019) 123–139.
[10] R. Djenadic, A. Sarkar, O. Clemens, C. Loho, M. Botros, V.S.K. Chakravadhanula, C. Kubel, S.S. Bhattacharya, A.S. Gandhi, H. Hahn, Multicomponent equiatomic rare earth oxides, Mater. Res. Lett. 5 (2017) 102–109.
[11] T. Dutta, K.-H. Kim, M. Uchimiya, E.E. Kwon, B.-H. Jeon, A. Deep, S.-T. Yun, Global demand for rare earth resources and strategies for green mining, Environ. Res. 150 (2016) 182–190.
[12] J. Gambogi, 2016 Minerals Yearbook—Rare Earths [Advance Release], December 2019 Ed, US Geological Survey, 2019.
[13] Y.F. Gomes, S. Ribeiro, M.C.B. Costa, F.V. Motta, Optimization of the process of obtaining RE_2O_3 from xenotime using statistical design, Ceramica 64 (2018) 79–85.
[14] X. Huang, H. Li, C. Wang, G. Wang, X. Xue, G. Zhang, Development status and research Progress in rare earth industry in China, Chin. J. Rare Met. 31 (2007) 279–288.
[15] A. Jordens, Y.P. Cheng, K.E. Waters, A review of the beneficiation of rare earth element bearing minerals, Miner. Eng. 41 (2013) 97–114.
[16] E. Kim, K. Osseo-Asare, Aqueous stability of thorium and rare earth metals in monazite hydrometallurgy: eh–pH diagrams for the systems Th–, Ce–, La–, Nd– (PO_4)–(SO_4)–H_2O at 25°C, Hydrometallurgy 113-114 (2012) 67–78.
[17] N. Krishnamurthy, C.K. Gupta, Extractive Metallurgy of Rare Earths, Second edittion CRC Press, Newyork, 2016.
[18] M. Kul, Y. Topkaya, I. Karakaya, Rare earth double sulfates from pre-concentrated bastnasite, Hydrometallurgy 93 (3) (2008) 129–135.
[19] I. Kursun, T.D. Tombal, M. Terzi, Solubility of Eskisehir thorium/rare earth ores in sulphuric and nitric acids, Physicochem. Problem. Min. Process. 54 (2) (2018) 476–483.
[20] L.Z. Li, X. Yang, China's Rare Earth Ore Deposits and Beneficiation Techniques, Proceedings of the 1st European Rare Earth Resources Conference, EURARE, Milos, Greece, 2014 28–39.
[21] H. Li, N. Zhao, G. Zhang, Y. Liu, Z. Long, X. Huang, A process of smelting monazite rare earth ore rich in Fe, Patent AU 2008286599, Grirem Advanced Materials Co., Ltd, 2010.
[22] C. Liao, S. Wu, F. Cheng, S. Wang, Y. Liu, B. Zhang, C. Yan, Clean separation technologies of rare earth resources in China, J. Rare Earths 31 (4) (2013) 331–336.
[23] J. Lucas, P. Lucas, T. Le Mercier, A. Rollat, W. Davenport, Chapter 4 - extracting rare earth elements from concentrates, rare earths: science, technology, production and use, Elsevier, Amsterdam, 2015 47–67.
[24] S. Massari, M. Ruberti, Rare earth elements as critical raw materials: focus on international markets and future strategies, Res. Policy 38 (1) (2013) 36–43.
[25] G. Nazari, J. Krysa, Assessment of various processes for rare earth elements recovery (I): a review, in: I. London, J. Goode, G. Moldoveanu, M. Rayat (Eds.),Proceedings of the 52nd conference of Metallurgsts (COM 2013), 1, , 2013.
[26] G. Ozbayoglu, M.U. Atalay, Beneficiation of bastnaesite by a multi-gravity separator, J. Alloys Compd. 303-304 (2000) 520–523.
[27] S. Peelman, Z.H.I. Sun, J. Sietsma, Y. Yang, Chapter 21 - leaching of rare earth elements: Review of past and present technologies, in: I. Borges de Lima, W. Leal Filho (Eds.), Rare Earths Industry, Elsevier, Boston 2016, pp. 319–334.
[28] L. Pietrelli, B. Bellomo, D. Fontana, M.R. Montereali, Rare earths recovery from NiMH spent batteries, Hydrometallurgy 66 (2002) 135–139.
[29] E.S. Pilkington, A.W. Wylie, Production of rare earth and thorium compounds from monazite, Part I. J. Soc. Chem. Industry 66 (11) (1947) 387–394.
[30] D.W. Pradip Fuerstenau, The role of inorganic and organic reagents in the flotation separation of rare-earth ores, Int. J. Miner. Process. 32 (1) (1991) 1–22.
[31] D.W. Pradip Fuerstenau, Design and development of novel flotation reagents for the beneficiation of mountain pass rare-earth ore, Min. Metallurg. Explor. 30 (1) (2013) 1–9.
[32] T. Qiu, H. Yan, J. Li, Q. Liu, G. Ai, Response surface method for optimization of leaching of a low-gradeionic rare earth ore, Powder Technol. 330 (2018) 330–338.
[33] F. Sadri, A.M. Nazari, A. Ghahreman, A review on the cracking, baking and leaching processes of rare earth element concentrates, J. Rare Earths 35 (8) (2017) 739–752.
[34] D. Schwartz, R. Gadiou, J.-F. Brilhac, G. Prado, G. Martinez, A kinetic study of the decomposition of spent sulfuric acids at high temperature, Ind. Eng. Chem. Res. 39 (7) (2000) 2183–2189.
[35] V.E. Shaw, Extraction of rare-earth elements from bastnaesite concentrate, US Department of the Interior - Bureau of Mines, Washington D.C, 1959.
[36] K.G. Shaw, M. Smutz, G.L. Bridger, A Process for Separating Thorium Compounds from Monazite Sands, Ames Laboratory, Iowa State College, Ames, Iowa, 1954.
[37] F. Soltani, M. Abdollahy, J. Petersen, R. Ram, M. Becker, S.M.J. Koleini, D. Moradkhan, Leaching and recovery of phosphate and rare earth elements from an ironrich fluorapatite concentrate: part i: direct baking of the concentrate, Hydrometallurgy 177 (2018) 66–78.
[38] S.F. Spear, M.J. Pyle, Apatite, monazite, and xenotime in metamorphic rocks, Rev. Mineral. Geochem. 48 (2002) 293–335.
[39] M.F. Sulaiman, An overview of the rare earth mineral processing industry in Malaysia, in: B. Siribumrungsukha, S. Arrykul, P. Sanguan Sai, T. Pungrassami, L. Sikong, K. Kooptarnon (Eds.), Proc. Int. Conf. Rare Earth Minerals and Minerals for Electronic Uses, Hat Yai, Thailand, January, Prince of Songkla University, Thailand 1991, pp. 389–395.
[40] T. Takeuchi, Hydrometallurgical treatment of acid-resistant ores, Transac. Natl. Res. Inst. Metals 18 (1) (1976) 31–41.
[41] R.W. Urie, Pilot plant production of rare earth hydroxides and thorium oxalate from monazite, J. Soc. Chem. Industry 66 (12) (1947) 437–439.
[42] R. Vijayalakshmi, S. Mishra, H. Singh, C. Gupta, Processing of xenotime concentrate by sulphuric acid digestion and selective thorium precipitation for separation of rare earths, Hydrometallurgy 61 (2001) 75–80.
[43] X. Wang, J. Liu, M. Li, H. Fan, Q. Yang, Decomposition reaction kinetics of Baotou RE concentrate with concentrated sulfuric acid at low temperature, Rare Metals 29 (2) (2010) 121–125.
[44] J. Wang, Z. Li, S. Zhang, S. Yan, B. Cao, Z. Wang, Y. Fu, Enhanced NH_3 gas-sensing performance of silica modified CeO_2 nanostructure based sensors, Sensors Actuators B Chem. 255 (2018) 862–870.
[45] Xia, C., Griffith, W., 2018. Direct oxalate precipitation for rare earth elements recovery. Patent, international publication number: WO2018195642.

[46] F. Xie, T.A. Zhang, D. Dreisinger, F. Doyle, A critical review on solvent extraction of rare earths from aqueous solutions, Min. Eng. 56 (2014) 10–28.
[47] A. Yorukoglu, A. Obut, I. Girgin, Effect of thiourea on sulphuric acid leaching of bastnaesite, Hydrometallurgy 68 (2003) 195–202.
[48] A.W. Zelikman, Metallurgy of Rare Metals, US NASA and NSF Publication, Washington, 1966 258.
[49] G. Zhang, W. Huang, Bastnaesite smelting process review, Rare Metals 21 (1997) 193–199.
[50] Y. Zhu, X. Zhai, L. Wang, Hydrothermal synthesis of $ln(OH)_3$ nanorods and the conversion to Ln_2O_3 (ln = Eu, Nd, Dy) nanorods via annealing process, J. Nanomater. (2013) 1–7.
[51] Z. Zhu, Y. Pranolo, C.Y. Cheng, Separation of uranium and thorium from rare earths for rare earth production – a review, Miner. Eng. 77 (2015) 185–196.